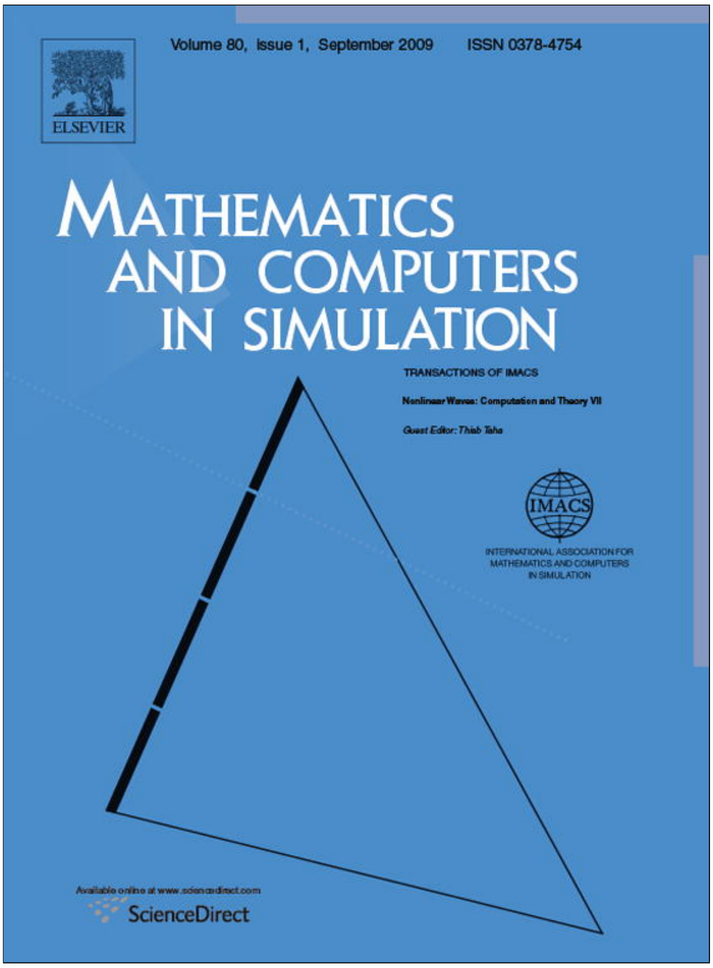
Volume 80, Issue 1, September 2009 ISSN 0378-4754
ELSEVIER
MATHEMATICS AND COMPUTERS IN SIMULATION
TRANSACTIONS OF IMACS
Nonlinear Waves: Computation and Theory VII
Guest Editor: Thiab Taha
IMACS
INTERNATIONAL ASSOCIATION FOR MATHEMATICS AND COMPUTERS IN SIMULATION
Available online at www.sciencedirect.com
ScienceDirect

Available online at www.sciencedirect.com
ScienceDirect
Mathematics and Computers in Simulation 80 (2009) 56–65
MATHEMATICS AND COMPUTERS IN SIMULATION
www.elsevier.com/locate/matcom

Identification of solitary-wave solutions as an inverse problem: Application to shapes with oscillatory tails

Christo I. Christov [a,*], Tchavdar T. Marinov [b], Rossitza S. Marinova [c,*]

[a] *Department of Mathematics, University of Louisiana at Lafayette, Lafayette, LA 70504-1010, USA*
[b] *Department of Natural Sciences, Southern University at New Orleans, 6801 Press Drive, New Orleans, LA 70126, USA*
[c] *Department of Mathematical & Computing Sciences, Concordia University College of Alberta, Edmonton, AB, T5B 4E4, Canada*

Available online 18 June 2009

Abstract

The propagation of stationary solitary waves on an infinite elastic rod on elastic foundation equation is considered. The asymptotic boundary conditions admit the trivial solution along with the solution of type of solitary wave, which is a bifurcation problem.

The bifurcation is treated by prescribing the solution in the origin and introducing an unknown coefficient in the equation. Making use of the method of variational imbedding, the inverse problem for the coefficient identification is reformulated as a higher-order boundary value problem. The latter is solved by means of an iterative difference scheme, which is thoroughly validated. Solitary waves with oscillatory tails are obtained for different values of tension and linear restoring force. Special attention is devoted to the case with negative tension, when the solutions have oscillatory tails.

PACS: 46.70.De; 46.70.Hg; 62.30.+d

Keywords: Solitary waves; Inverse problems; Coefficient identification; Method of variational imbedding

1. Introduction

The solitary wave (localized wave with permanent character) was first observed by John Scott Russell on the surface of a shallow water layer (a canal near Edinborough) and the theory of the solitary waves was developed by Boussinesq [1] to explain his observations. The work of Boussinesq introduced a new paradigm in which the existence of permanent waves in nonlinear systems is the result of the balance between nonlinearity and dispersion. Under the assumption of slow evolution in the frame moving with the center of the solitary wave, Boussinesq's equation can be reduced to the famous Korteweg and deVries equation (KdV) for which Zabusky and Kruskal [19] discovered numerically wave solutions with particle-like behavior which they called the *solitons*.

Later on, the Boussinesq equation was shown to apply to the continuous limit of atomic lattices [18] (see, e.g., [6]) and to the flexural deformations of elastic rods. Solitons on elastic rods have been studied for different models and by different techniques (see, e.g. [9,16], and the monograph [14]). For the more fundamental issues about the connection of solitary wave problems to homoclinic bifurcation, see the illuminating review [3]. However, the investigations are

* Corresponding author.
E-mail addresses: christov@louisiana.edu (C.I. Christov), marinov@louisiana.edu (T.T. Marinov), rossitza.marinova@concordia.ab.ca (R.S. Marinova).

0378-4754/$36.00 © 2009 IMACS. Published by Elsevier B.V. All rights reserved.
doi:10.1016/j.matcom.2009.06.019

predominantly focused on solitons with monotonically decaying tails which take place when the tension in the rod is positive. Completely new phenomena are observed if the tension is negative (the rod is axially compressed). For finite rods, this is the famous Euler problem of buckling (see, e.g. [20]), but for infinitely long rods (or atomic chains), the problem with negative tension is not correct in its original posing, and becomes a tractable mathematical model only if a linear restoring elastic force is incorporated — force from the elastic foundation. This paper deals with the stationary solitary waves propagating in an elastic rod on elastic foundation. The problem does not admit analytical solution and has to be approached numerically.

The problem of bending of elastic rods on elastic foundation has important applications as well, e.g., in railroads [10], conveyers, large-scale floating structures [17]. The dynamical problem is discussed in [13]. The problem of *buckling* of an infinite rod subjected to restoring transversal force (e.g., elastic foundation) is much less studied.

Apart from the engineering applications, the problem of buckling of nonlinear infinite rod on elastic foundation with restoring force is important also from fundamental point of view. The above mentioned interplay between the negative membrane tension, the momentum stresses and the restoring force from the elastic foundation can sustain localized solitary waves. In the classical Boussinesq equation (rod with positive tension), the solitary waves pass through each other during their interaction because of the positive force acting between the two Quasi Particles (QPs) that are the two solitons. For the equation governing the flexural deformation of an elastic rod on elastic foundation (EREFE), when the membrane tension is negative, the interaction force will be repelling, and the dynamics of the QPs will be rather different. The only other system where repelling interaction is observed is the case of so-called soliton-soliton interaction in sine-Gorden equation (see [8] for details). Before attacking the dynamical problem, one needs reliable method and algorithm for computing the shape of a stationary propagating QP. The shapes of the solitary waves of EREFE are much more intricate and for some values of the governing parameters they may have non-monotone shapes. In the present paper we propose a numerical technology for finding the localized solutions of EREFE.

The numerical computation of solitary-wave solutions faces two main challenges. The first difficulty arises from the fact that the original problem is posed over an infinite interval. This means that any truncation of the computational domain will inevitably entail dealing with numerical artifacts connected with the truncation of the region. The most successful techniques among the available from the literature, are those which make use of coordinate transformations or spectral expansion or both [2]. Application of a specialized complete orthonormal (CON) system of functions for creating Galerkin spectral techniques for the Boussinesq type of equation is elaborated in [4] and the works cited therein. The results obtained there show that a spectral method with well tuned basis function is a very efficient approach to problems in infinite domains. Yet, the truncation of the infinite interval with finite difference discretization is not the hardest hurdle and it gives satisfactory results when carefully implemented. The second, and sometimes harder difficulty, is that the existence of solitary wave is the result of a bifurcation. Due to the nature of asymptotic boundary conditions for the decay at infinity, the system under consideration always possesses a trivial solution. It takes special measures to avoid the trivial solution when using an iterative method, since, as a rule, the trivial solution is a very strong attractor. In many instances, the problem of finding the nontrivial amplitude of the bifurcating solution is akin to the problem of coefficient identification. The above outlined difficulties are much harder to deal with when the solution has nonmonotone tails and when the interval where it is well separated from zero (the 'support'), is large.

A new approach to creating effective algorithms for treating the bifurcation problem for localized solutions was originated in [5] and applied to finding the homoclinic solution of Lorentz equations [11]. The Rayleigh number for which the homoclinic solution first appears, was identified as an unknown coefficient using the so-called method of variational imbedding (MVI). The latter consists in replacing the original (inverse) problem by the Euler–Lagrange equations for minimization of a quadratic functional of the governing equations. In [7], MVI was successfully applied to finding the shape of the wave and the phase speed for which a solitary wave exists for an equation governing Bénard–Marangoni convection. Recently (see [12]), MVI allowed obtaining numerically the solitary-wave solutions of the sixth-order generalized Boussinesq equation, or 6GBE (see [6] for the derivation of that equation).

The equation governing the flexural deformation of an elastic rod on elastic foundation (EREFE) is only of fourth order, but because of the presence of the linear restoring force, it exhibits some of the phenomenology of the 6GBE, especially when the nonmonotonic shapes are concerned. Yet, the linear term presenting the restoring force, changes qualitatively the equation for the stationary waves. The ODE to which the problem reduces in the moving frame can no longer be integrated, and the nonlinearity in EREFE is harder to treat than for the 6GBE. Hence, it is important to investigate numerically the solitary waves of EREFE, and the present paper is devoted to doing that using MVI.

2. Posing the problem

In terms of dimensionless variables, the governing equation of the transverse deflections of an elastic rod on elastic foundation equation reads (see, e.g., [13])

$$u_{tt} = [\sigma u - u^2 + \gamma_1 u_{tt} - \gamma_2 u_{xx}]_{xx} - \delta u, \quad \delta > 0, \tag{1}$$

where σu_{xx} is the term responsible for the tension acting along the axis of the rod. When the rod is subjected to axial extension, then $\sigma > 0$ and $c = \sqrt{\sigma}$ is the characteristic speed of the transverse (shear) waves. When $\sigma < 0$, the rod is subjected to axial compression, and the well known Euler buckling can take place. When an infinite rod undergoes buckling, the amplitude of the deformation can become infinite. This effect is mitigated by the linear restoring force from the foundation, $-\delta u'$ which arises when the rod is firmly connected to an elastic foundation. In the case when $\sigma < 0$, one can formally write $c = \sqrt{-\sigma}$, but then c does not have the physical meaning of a characteristic speed. In other words, the equation is no longer hyperbolic, in the absence of the stiffness term, $\gamma_2 u_{xxxx}$. Finally, the term $\gamma_1 u_{ttxx}$ accounts for the so-called rotational inertia. As far as stationary waves are the scope of the investigation, the rotational inertia merely changes the numerical value of the coefficient of the fourth derivative, and we do not consider it in what follows. The coefficient of the nonlinear term can be rescaled and for this reason it is taken to be equal to unity. Similarly, the coefficient γ_2 can be taken equal to unity because it can be rescaled on infinite intervals.

A critical new phenomenology arises when the rod is subjected to a reaction force from the elastic foundation. Since both the momentum (the fourth derivative) and the restoring-force from the foundation (the linear term), are represented by negative definite terms in Eq. (1), the problem can be mathematically correct even if the tension (the coefficient of the second-derivative term) is negative. Without the linear term, the problem with negative tension can never be correct in an infinite domain, because in this case one can always find a long enough wave for which the second derivative dominates the fourth derivative. Note, that the situation for short waves is reversed: the fourth derivative dominates the second derivative and hence the short waves are stable. This means that new physical phenomena connected with the negative tension can be deducted from the model presented by Eq. (1). Concerning the solutions of type of localized waves (solitary waves), the negative tension changes the potential of interaction of the solitary waves. The result of this change can be that the solitary waves repel each other, rather than attract themselves (as it is in the case with positive tension). The significance of the sign of the interaction potential is discussed in detail in [8] where the interaction of kinks of sine-Gordon equation are shown to be rather different form the interactions of the antikinks of the same equation.

The first step towards understanding the soliton dynamics governed by Eq. (1) is to find the shapes of the waves that are stationary in a frame moving with speed v, when the solution depends only on the variable $\xi = x - ct$. Then Eq. (1) is reduced to the following ODE

$$-\delta u - (u^2)_{\xi\xi} + \beta u_{\xi\xi} - u_{\xi\xi\xi\xi} = 0, \tag{2}$$

where $\beta = \sigma - v^2 = \pm c^2 - v^2$. We are looking for non-trivial solution of Eq. (2) with $u(\xi) \to 0$ when $\xi \to \pm\infty$.

We begin with mentioning the obvious symmetry of the solution in the absence of loading force. Namely, if $u(\xi) \neq 0$ is a solution of Eq. (2), the function $u(-\xi)$ is also a solution, i.e. the solution is an even function, satisfying the condition $u(\xi) = u(-\xi)$. This fact allows us to consider the problem on the half-line with boundary conditions (b.c.) at $\xi = 0$

$$u'(0) = 0, \quad u'''(0) = 0, \tag{3}$$

to which one has to add the requirement that $u(0) \neq 0$ in order to eliminate the trivial solution. A way to do this is to impose the following condition

$$u(0) = \chi, \tag{4}$$

where $\chi \neq 0$ is an unknown constant.

3. Introducing an unknown coefficient

The most important feature of a problem with asymptotic boundary conditions is that scaling the dependent variable does not change the nature of the boundary value problem. Let us introduce a new function $w(\xi) = u(\xi)/\chi$, and cast

Eq. (2) into the form

$$\mathcal{A}(w, \chi) \equiv -\delta w - \chi(w^2)_{\xi\xi} + \beta w_{\xi\xi} - w_{\xi\xi\xi\xi} = 0, \tag{5}$$

For the new function $w(\xi)$, we have the following boundary conditions

$$w(0) = 1, \quad w'(0) = 0, \quad w'''(0) = 0, \tag{6}$$

$$w(\xi) \to 0, w'(\xi) \to 0 \quad \text{when} \quad \xi \to \infty. \tag{7}$$

Thus, the problem with unknown constant χ in the boundary condition is reformulated as a problem of identifying an unknown coefficient χ from over-posed boundary data. If χ is thought of as known, then the problem is overdetermined, i.e., the function may not be able to satisfy all of the boundary conditions. However, the problem can have a solution if χ is considered as one of the unknowns. Under certain natural conditions, it is possible to find a constant χ such that the equation for $w(\xi)$ has solution and this solution also satisfies the boundary conditions. In such a case we say that the pair (w, χ) constitutes a solution to the problem (5)–(7).

4. Method of variational imbedding (MVI)

In order to solve the above formulated problem of coefficient identification, we use the so-called method of variational imbedding (MVI), which consists of replacing the original problem by a problem of minimization of the following functional

$$\mathcal{I}(w, \chi) = \int_0^\infty [\mathcal{A}(w, \chi)]^2 dx \to \min, \tag{8}$$

where $\mathcal{A}(w, \chi)$ is defined in (5), w satisfies the boundary conditions Eq. (6), (7), and $\chi \neq 0$ is an unknown constant. The functional $\mathcal{I}(w, \chi)$ is a quadratic and homogeneous function of $\mathcal{A}(w, \chi)$ and hence it attains its absolute minimum if and only if $\mathcal{A}(w, \chi) \equiv 0$. In this sense, there is one-to-one correspondence between the solution of the original problem and the minimization problem.

Since the problem is nonlinear it has to be linearized it in order to solve it numerically. This can be done after the Euler–Lagrange equations are derived, or, alternatively, the integrand in (8) can be linearized considering the nonlinear term as the product $q(x)w(x)$ where function q is thought of as known (say, this is the same function w, but taken from the previous iteration, i.e., $q(\xi) = w(\xi)$). Using the latter approach to linearization, we consider the problem of minimization of the following functional

$$\mathcal{I}_1(w, \chi) = \int_0^\infty [F(\xi)]^2 dx \to \min, \quad F(\xi) \equiv -\delta w - \chi(qw)_{\xi\xi} + \beta w_{\xi\xi} - w_{\xi\xi\xi\xi} \tag{9}$$

where $F(\xi)$ is the residual of the given equation, and $q(\xi)$ is the above introduced known function. The Euler–Lagrange equation for the unknown function $w(\xi)$ reads

$$\begin{aligned} &\delta[F(\xi)] + (2\chi q - \beta)\frac{d^2}{d\xi^2}[F(\xi)] + \frac{d^4}{d\xi^4}[F(\xi)] \\ &\quad \equiv \delta[\lambda w + \chi q w + \beta w_{\xi\xi} + w_{\xi^4}] + (2\chi q - \beta)\frac{d^2}{d\xi^2}[\lambda w + \chi q w + \beta w_{\xi\xi} + w_{\xi^4}] \\ &\qquad + \frac{d^4}{d\xi^4}[\lambda w + \chi q w + \beta w_{\xi\xi} + w_{\xi^4}] = 0. \end{aligned} \tag{10}$$

This equation is of the eight order if $F(\xi)$ is substituted in Eq. (10). However, we do not make use of the eight-order equation. Rather we solve the system of two coupled Eqs. (9) and (10), each of them of the fourth order.

The boundary condition in the origin for the unknown $F(\xi)$ stems from the fact that it is the residual of the original equation, Eq. (5), so that it has to be zero for $\xi = 0$. Thus

$$F(0) = 0. \tag{11}$$

Fig. 1. Grid pattern.

To the above boundary condition, one has to add also the asymptotic boundary conditions (a.b.c.):

$$F(\xi) \to 0, \quad F'(\xi) \to 0, \quad \text{when} \quad \xi \to \infty. \tag{12}$$

The gist of MVI is that an explicit equation for the unknown constant χ can be derived. After some manipulations, the Euler–Lagrange equation for the constant χ adopts the form:

$$\chi = -\frac{\int_0^\infty (qw)_{\xi\xi}(\delta w - \beta w_{\xi\xi} + w_{\xi\xi\xi\xi})d\xi}{\int_0^\infty [(qw)_{\xi\xi}]^2 d\xi}. \tag{13}$$

5. Difference scheme and algorithm

For the numerical treatment of the imbedding problem we introduce a certain large number ξ_∞, called ‘actual infinity’, and solve the problem in the interval $\xi \in [0, \xi_\infty]$, using finite difference approximations. An important feature of the scheme is that Eqs. (9), (10) must be solved as a coupled system. Iterative decoupling of the system is not possible because five boundary conditions are imposed on the function w, while for F only three are present. In other words, at $\xi = 0$ we have three boundary conditions for w and only one for F. For this reason we construct an algorithm for the solution of the problem that solves the algebraic system of equations simultaneously. We use a staggered grid (see Fig. 1), which allows us to obtain second-order difference approximations on a four-point stencil of the different derivatives involved in the boundary conditions. Now, to preserve the coupling of the system we introduce a new difference function, Φ_j which is composed in a hopscotch manner by the values of the two difference functions, w_i, F_i, namely

$$\Phi_{2i-1} = w_i, \quad \Phi_{2i} = F_i, \quad \text{for} \quad i = 1, 2\ldots, n. \tag{14}$$

Thus, we arrive at a nine-diagonal algebraic system for a vector of dimension $2n$. The determinant of this system is of order $O(h^4)$ which gives advantage over solving the eight-order equation, because for the latter the determinant is of order of $O(h^8)$. Because of the banded structure of the matrices, efficient algorithms for the inversion can be employed.

We approximate the integrals for χ in Eq. (13) using the so called ‘extended midpoint rule’ (see e.g., [15]). The local truncation error is $O(h^2)$ and we can prove that the global error is of the same order, $O(h^2)$.

Different ways of organizing the iterations can be followed, and we did actually implement more than one. The most robust turned out to be the algorithm involving, what we call, ‘internal iterations’. The gist of this approach is that for a given coefficient χ we conduct iterations for the difference system approximating Eq. (9), (10), by iterative replacing of q by the computed w until convergence is reached in the sense that q stops changing during the iterations. Before χ finds its correct value, what we obtain is not the solution of the problem from Eq. (5), but only a current approximation. In other words, one iteration is completed after the internal iterations converge for this specific value of χ. Then we use the integral equality, Eq. (13) to compute the new value of the coefficient χ and begin a new cycle of internal iterations for w.

The algorithm is organized as follows

(i) The eight-order boundary value problem (9) and (10) for w is solved with given $\chi = \chi^n$ and q.

(ii) If

$$\max|w - q| < \varepsilon \max|w|, \tag{15}$$

then we proceed to (3), otherwise q is replaced by w and then the algorithm returns to (1).

(iii) With the newly computed w, the coefficient χ is evaluated from Eq. (13) and then the algorithm returns to (i).

(iv) When

$$\max|\chi - \chi^n| < \varepsilon \max|\chi|, \tag{16}$$

the calculations are terminated and the obtained w, χ are considered as the sought solution. Otherwise, the obtained values are considered as the functions at the new iteration stage, $w^{n+1} \equiv w$, $\chi^{n+1} \equiv \chi$, and the algorithm is returned to (i) after stepping up the index $n := n+1$.

Note, that for the calculations presented here, we use $\varepsilon = 10^{-10}$.

6. Validations

In order to validate our scheme and algorithm we consider a simplified case with $\delta = 0$ and a coefficient of the nonlinear term equal to $-1/6$. We also select $\beta = 4$. For these parameters the well known *sech*-solution exists, namely

$$w_{\mathrm{anl}}(\xi) = 6\,\mathrm{sec}\,h^2(\xi), \tag{17}$$

which means that for the unknown coefficient in MVI we have the following target $\chi_{\mathrm{anl}} = 6$.

First we investigate the role of the so-called "actual infinity", ξ_∞, at which the originally unbounded region is truncated for the purposes of the finite-difference implementation of MVI. To this end, we begin the validations of our scheme with the case with analytical solution, Eq. (16). We set the spacing at $h = 0.05$, i.e., when a larger value for ξ_∞ is considered, a larger number of grid points is used. This way the truncation error is kept the same for all diffrent ξ_∞. In the range for the independent variable where the magnitude of the function is larger than 5×10^{-5}, the solution complies with the truncation error for all the selected values of ξ_∞. Increasing ξ_∞ mostly increases the actual length of the interval where the above condition is satisfied. A good representation of the solution is obtained for $\xi_\infty \geq 40$. Since in the case of nonmonotone tails the support of the solution can become larger, we played with different ξ_∞. In most of our calculations we set $\xi_\infty = 60$ but, when necessary, we use 'actual infinities' as large as $\xi_\infty = 200$.

The next important validation is connected with the local and global truncation errors, which are supposed to be of the order of $O(h^2)$. For the case with the analytical solution, we compute the solution with a given spacing and subtract the analytical solution, Eq. (16), to get the pointwise error. We consider also a case for which no analytical solution is available. In this case we compute the distance between two different solutions for which the spacings are in the ratio 2:1. In this test we fix $\xi_\infty = 60$ and vary the spacing: $h = 0.1$, 0.05, 0.025, 0.0125. Fig. 2 presents the computed errors.

The left panel shows the errors for the case with analytical solution, while the right panel depicts the error for the case without analytical solution. It is seen from the figure that in both cases the absolute error is concentrated around the origin, and that it is of order of $O(h^2)$, because the ratio between the maxima is close to four for two error curves presenting the difference between the solutions obtained with spacings related as 2:1.

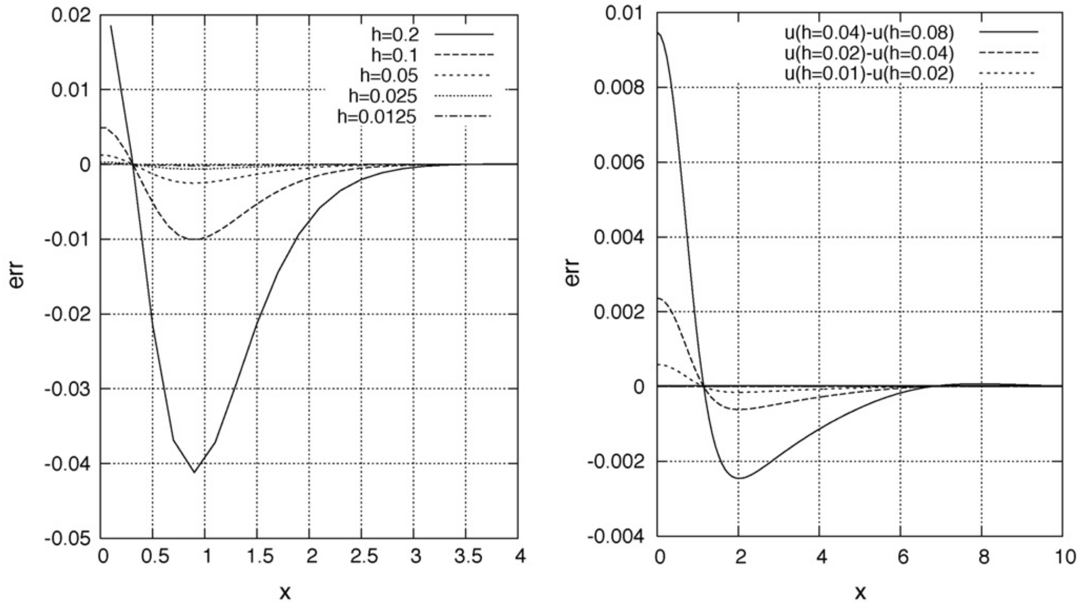

Fig. 2. Pointwise error. Left panel: difference between MVI solution and analytical solution, Eq. (16). Right panel: difference between two MVI solutions with spacings in ratio 2:1.

Table 1
Truncation error and convergence.

(a) Comparison with the analytical solution, Eq. (17), for the coefficient χ and the profile, w.

h	χ	r_h^χ	$\|\|w_h - w_{\text{anl}}\|\|_2$	r_h^w
0.2	5.95897	–	0.03807	–
0.1	5.98993	2.02746	0.00924	2.04278
0.05	5.99749	2.00618	0.00228	2.01692
0.025	5.99937	1.99947	0.00056	2.00812
0.0125	5.99984	1.96551	0.00014	2.01738

(b) Comparison of the errors between solutions on different grids.

h	$\|\|w_h - w_{h/2}\|\|_2$	r_h^w
0.16	0.0094700	–
0.08	0.0023618	2.003477625
0.04	0.00059032	2.000317675
0.02	0.000014755	–

The above statement can be quantified introducing the convergence rate according to the standard formula

$$r_h^\chi = \log_2 \frac{||\chi_{2h} - \chi_{\text{anl}}||_2}{||\chi_h - \chi_{\text{anl}}||_2}, \quad \text{and} \quad r_h^w = \log_2 \frac{||w_{2h} - w_{\text{anl}}||_2}{||w_h - w_{\text{anl}}||_2}, \tag{18}$$

where w_{anl}, χ_{anl} is the analytical solution. Respectively, when no analytical solution is available, then

$$r_h^\chi = \log_2 \frac{||\chi_{2h} - \chi_h||_2}{||\chi_h - \chi_{h/2}||_2}, \quad \text{and} \quad r_h^w = \log_2 \frac{||w_{2h} - w_h||_2}{||w_h - w_{h/2}||_2}. \tag{19}$$

The two panels of Table 1 present the quantitative details about the convergence of χ and w for the the cases shown in the two panels of Fig. 2. The results presented in Table 1 clearly demonstrate that the convergence for the coefficient is quadratic. We also mention that the variational functional is of order of magnitude smaller than the truncation error.

7. Results and discussion

For the new equation considered in this work, the new phenomenology is associated with the term accounting for the linear restoring force from the elastic foundation. As already mentioned, the presence of the linear term δu allows for existence of localized solutions even if the second-derivative term is negative. For this reason we begin with investigating the dependence of the profile of the localized wave on the parameter δ. Quantitatively speaking, a larger linear restoring force must lead to larger deflections of the rod. Indeed, as shown in Fig. 3, larger δ entails a larger amplitude of the solitary wave.

In the left panel of the figure we present the profiles for a positive $\beta = 0.5$, while in the right panel are presented the results for negative $\beta = -0.5$. It is interesting to note that, qualitatively speaking, the role of δ is similar in the two cases, but the waves are taller for $\beta > 0$ for the same values of δ.

Looking closer into the mechanism of creation of a localized solution, one can say that the tails of the solution (extending either to $+\infty$ or $-\infty$) satisfy the linearized equation. It is also clear that the same solution of the linearized equation cannot be valid at both extremes. Rather, at each infinity one has a different tail, each of which tails is a solution of the linearized equation. In a sense, the nonlinearity plays important role around the center of the localized wave and acts to 'mold' the solution so that the latter smoothly leaves the linear solution valid at the left extreme, $\xi \to -\infty$, and transforms into the other linear solution valid for $\xi \to \infty$. Hence, one can have an *a-priori* estimate of the asymptotic behavior of the solution based on the solutions of the linearized equation. In particular, we consider solutions of the type e^{kx}. The dispersion relation for this kind of stationary waves reads

$$k^4 - \beta k^2 + \delta = 0, \Rightarrow k_{1,2,3,4} = \pm \frac{1}{\sqrt{2}} \sqrt{\beta \pm \sqrt{\beta^2 - 4\delta}}. \tag{20}$$

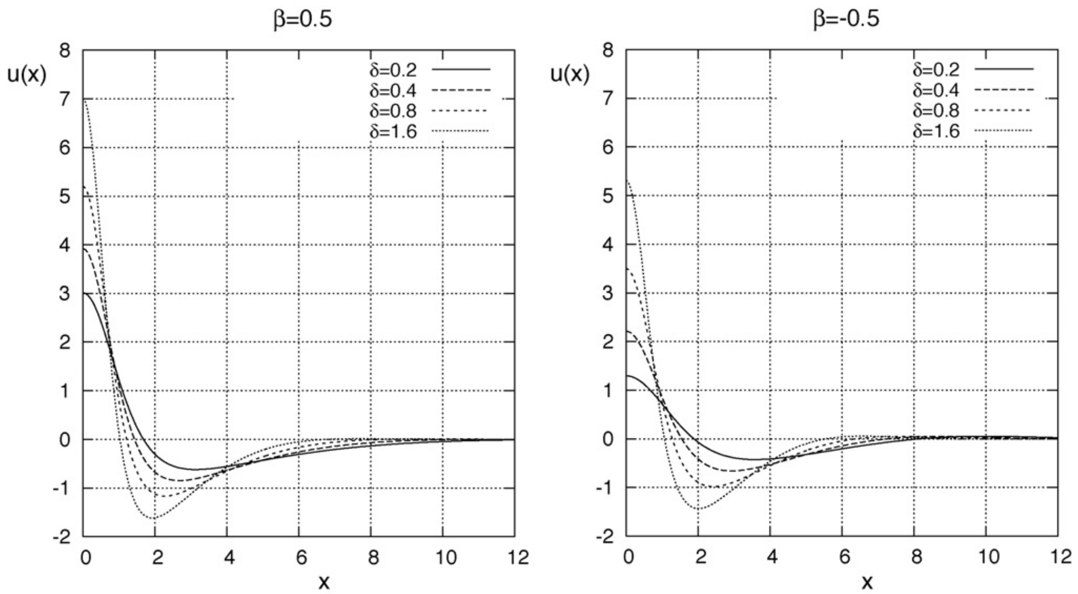

Fig. 3. The profile of the solution for different δ when non-monotone shapes are possible. Left panel: $\beta = 0.5$. Right panel: $\beta = -0.5$.

when $\beta^2 > 4\delta$, the expression under the radical is real. For $\beta > 0$ this expression is also positive, which means that the solution is a monotone function of x that decays either at $+\infty$ or $-\infty$. Consider here the case $|\beta| < 2\sqrt{\delta}$ when the inner radical in Eq. (19) is negative, i.e., the outer radical is a complex function. Then, one can write

$$k_{1,2,3,4} = \pm\sqrt{\frac{1}{2}\left(\sqrt{\delta} + \frac{1}{2}\beta\right)} \pm i\sqrt{\frac{1}{2}\left(\sqrt{\delta} - \frac{1}{2}\beta\right)}, \tag{21}$$

which means that if δ and/or β are increased, the decay of the solution will become faster. The wave length of the oscillations, however, depends on the difference between $\sqrt{\delta}$ and $\beta/2$ and it can increase if the said difference decrease, regardless of the absolute magnitudes of δ and β.

The solution presented in Fig. 4 is for two different δ and several β's. As expected, the localization of the solutions for $\beta > 0$ is tighter for $\delta = 1$ than for $\delta = 0.1$. Respectively, the wave-length is generally longer in the case of $\delta = 0.1$ in comparison to $\delta = 1$. At the same time, the solution in the right panel of Fig. 4 spans a larger region, i.e., its support is

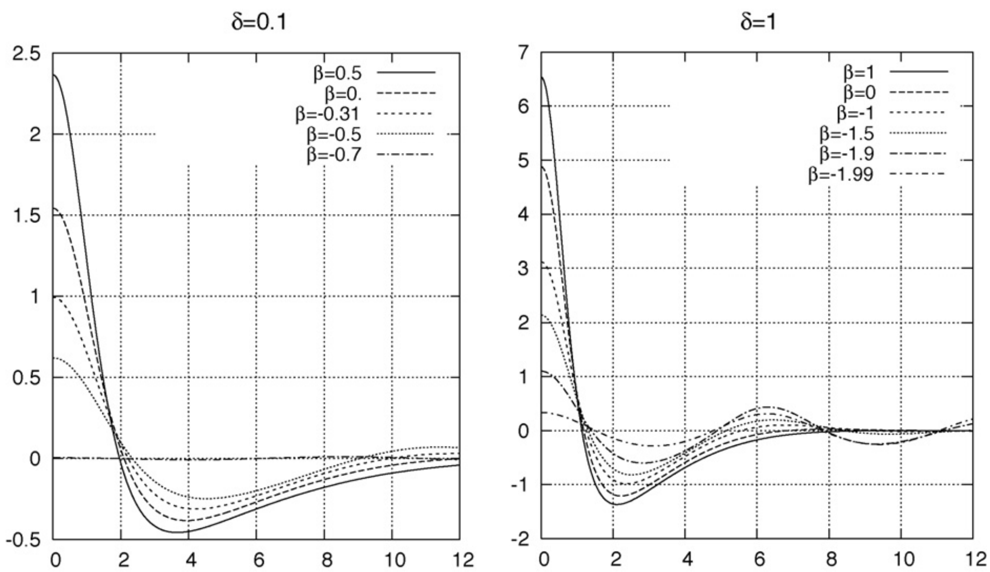

Fig. 4. Evolution of the wave profile with β for two different δ.

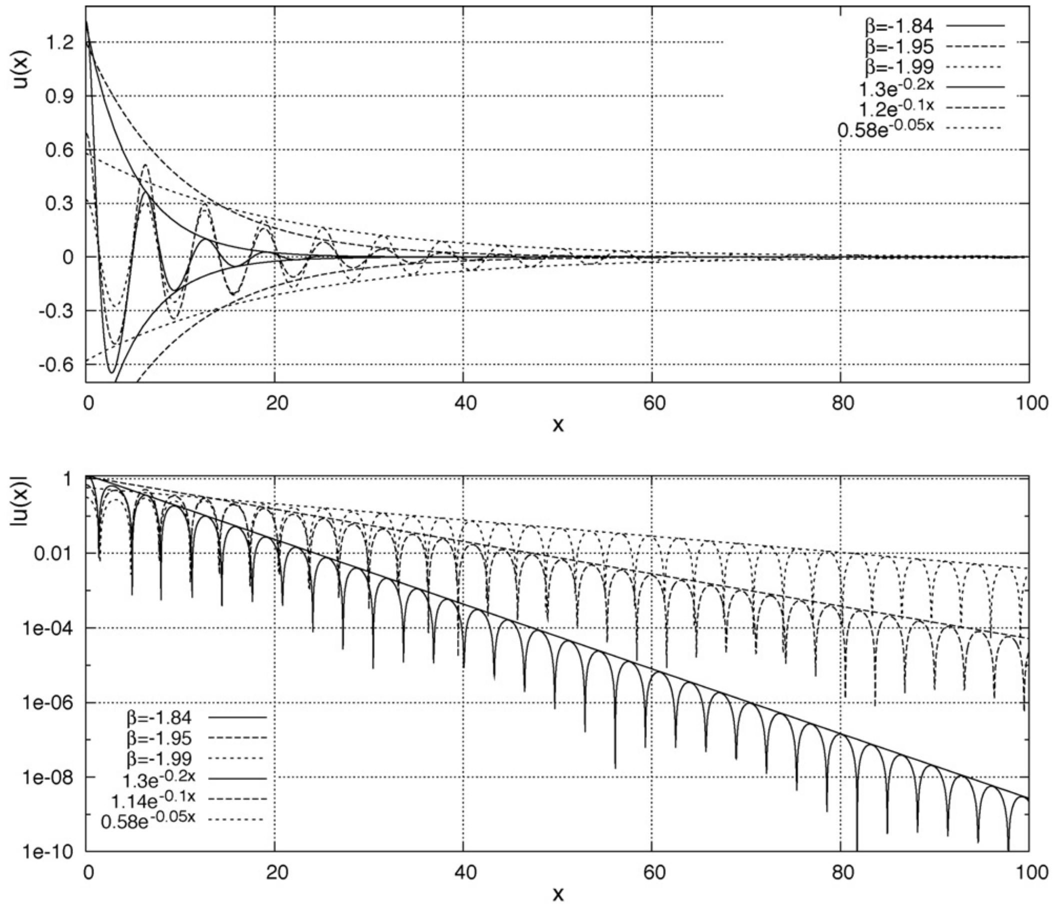

Fig. 5. Solutions with oscillatory tails near the threshold of nonexistence and best fits with exponents of the type of $A\exp\left(-0.5\sqrt{|\beta^2-4\delta|}\right)$.

larger, despite of the fact that the wave-length is somewhat shorter. The situation is reversed to certain extent for $\beta<0$ when the decay becomes slower for larger $|\beta|$, while the wave number increases (the oscillations become shorter).

To investigate this behavior in greater detail, we choose for definiteness $\delta=1$ and consider values of β that are close to the threshold of existence, namely $|\beta|=\sqrt{4\delta}=2$. As already mentioned, if we take $\beta>2\sqrt{\delta}>0$, all four solutions of Eq. (19) are real, which means that the tails are monotone and dominated by the wave numbers that have smaller absolute value. The other case, when $\beta<0$, and $|\beta|\lessapprox 2$ can be treated if we assume that $\beta=-2+\varepsilon^2$. Then for the wave numbers and for the solutions of the linearized equation, we get

$$k_{1,2,3,4}=\pm\frac{i}{2}\mp\frac{\varepsilon}{2}\quad e^{-(\varepsilon/2)x}\left(A\cos\frac{x}{2}+B\sin\frac{x}{2}\right),\quad e^{(\varepsilon/2)x}\left(C\cos\frac{x}{2}+D\sin\frac{x}{2}\right). \tag{22}$$

The first of these solutions represents a spatially oscillating stationary in the moving frame wave that decays for $x\to\infty$, whereas the second one is the same kind of wave that decays at $x\to-\infty$.

The solution for three negative β's is presented in Fig. 5. Since a larger spatial extent of the solution is expected, we use a larger actual infinity, $\xi_\infty=200$ for the tests shown in Fig. 5. The enlargement of the support with the increase of the modulo of β is clearly seen. The formula for the asymptotic decay of the tails, Eq. (21), is splendidly confirmed by the juxtaposition to exponential functions with appropriate exponents. For $\beta=-1.99$, the decay is so slow, that one can liken the solution to a harmonic function, which is exactly the solution from Eq. (21) with $\varepsilon=0$. Success in the latter very hard case testifies to the reliability of the created here numerical scheme on the one hand, and presents a new information about the solitary-wave solutions of EREFE — on the other.

8. Conclusions

In this work we have investigated the stationary solitary waves propagating on an elastic rod when the latter is subjected to linear restoring force from an elastic foundation. Stationary in the moving frame waves are considered and a special attention is paid to the case when the term with the second derivative can have negative coefficient. This happens either when the tension is negative or when the phase speed of the wave exceeds the characteristic speed in the case of positive tension. The new solitary waves have shapes, which are rather different from the ubiquitous 'humps' and exhibit oscillatory tails.

In order to investigate the shapes numerically we apply the so-called method of variational imbedding (MVI) and replace the original bifurcation problem with a higher-order boundary value problem (b.v.p.) for the Euler–Lagrange equations for minimization of the quadratic functional of the original equation. MVI gives us also an explicit integral equation for the unknown coefficient related to the unknown height of the wave in the origin. The new b.v.p. is solved by means of an iterative difference scheme on a staggered grid. The scheme is thoroughly validated and shown to have second-order truncation error.

Making use of the developed scheme and algorithm, a variety of solitary waves with oscillatory shapes are obtained numerically. In general, the larger values of the force from the foundation, entail larger amplitudes of the waves, but the specific shapes are influenced also by the coefficient of the second derivative. The strongly nonlinear cases are presented graphically. It is also shown that near the threshold of non-existence, the solitary waves span much larger support and their amplitudes decrease, approaching thus the limit of linear harmonic waves.

Acknowledgement

The work of R. Marinova was partially supported by a grant from MITACS.

References

[1] J. Boussinesq, Théorie des ondes et des remous qui se propagent le longd'un canal rectangulaire horizontal, en communiquant au liquide contenu dans ce canal des vitesses sensiblement pareilles de la surface au fond, J. Math. Pure Appl. 17 (1872) 55–108.

[2] J.P. Boyd, Chebishev and Fourier Spectral Methods, second ed., Dover, New York, 2001.

[3] A. Champneys, Homoclinic orbits in reversible systems and their applications in mechanics, fluids and optics, Physica D 112 (1–2) (1998) 158–186.

[4] M.A. Christou, C.I. Christov, Localized waves for the regularized long wave equation via a Galerkin spectral method, Math. Comp. Simulat. 69 (2005) 257–268.

[5] C.I. Christov, A method for identification of homoclinic trajectories, in: Proc. 14-th Spring Conf., Sunny Beach, Union of Bulg. Mathematicians, Sofia, Bulgaria, 1985.

[6] C.I. Christov, G.A. Maugin, M.G. Velarde, On the well-posed Boussinesq paradigm with purely spatial higher-order derivatives, Phys. Rev. E 54 (1996) 3621–3638.

[7] C.I. Christov, M.G. Velarde, On localized solutions of an equation governing Bénard-Marangoni convection, Appl. Math. Modell. 17 (1993) 311–320.

[8] I. Christov, C.I. Christov, Physical dynamics of quasi-particles in nonlinear wave equations, Phys. Lett. A 372 (2008) 841–848.

[9] P.A. Clarckson, R.J. Le Veque, R. Saxton, Solitaty-wave interactions in elastic rods, Stud. Appl. Math. 75 (1986) 95–122.

[10] S.L. Grassie, R.W. Gregory, D. Harrison, K. Johnson, The dynamic response of railway track to high frequency vertical excitation, J. Mech. Engin. Sci. 24 (1982) 77–90.

[11] E.N. Lorenz, Deterministic nonperiodic flow, J. Atmos. Sci. 20 (1) (1963) 130141.

[12] T.T. Marinov, C.I. Christov, R.S. Marinova, Novel numerical approach to solitary-wave solutions identification of Boussinesq and Korteweg-De Vries Equations, Int. J. Bifur. Chaos 15 (2005), 557-265.

[13] A.D. Myshkis, P.M. Belotserkovskiy, On resonance of an infinite beam on uniform elastic foundation, ZAMM Z. Angew. Math. Mech. 79 (1999) 645–647.

[14] A.V. Porubov, Amplification of Nonlinear Strain Waves in Solids, World Scentific, New Jersey, 2003.

[15] W.H. Press, S.A. Teukolsky, W.T. Vetterling, B.P. Flannery, Numerical Recipes: The Art of Scientific Computing, Cambridge University Press, 2007.

[16] A.M. Samsonov, Nonlinear waves in elastic waveguides Courses and Lectutres of Internatinal Centre for Mechanical Sciences, 341, Springer, New York, 1994.

[17] H. Suzuki, K. Yoshida, K. Iijima, A consideration of the structural design of a large-scale floating structure, J. Mar. Sci. Technol. 1 (1996) 255–267.

[18] M. Toda, Vibration of chain with nonlinear interaction, J. Phys. Soc. Jpn. 22 (1967) 431–436.

[19] N.J. Zabusky, M.D. Kruskal, Interaction of 'solitons' in collisionless plasma and the recurrence of initial states, Phys. Rev. Lett. 15 (1965) 57–62.

[20] F. Ziegler, Mechanics of Solids and Fluids, Springer, 1998.